Research Square

Preprints are preliminary reports that have not undergone peer review.
They should not be considered conclusive, used to inform clinical practice,
or referenced by the media as validated information.

Resting-State MEG Functional Connectivity Changes in Lumbar Spinal Stenosis: A Multi-Band wPLI and Machine Learning Study

Geng Zhao
Beihang University
Zhuang Miao
Beihang University
Xiaoxiong Wang
Qilu Hospital of Shandong University
Hongwei Wang
Shandong First Medical University
Shiqiang Zheng
Beihang University
Xinyu Liu
Qilu Hospital of Shandong University
Xu Zhang
zhang_xu@buaa.edu.cn

Beihang University

Article

Keywords: Lumbar Spinal Stenosis, Magnetoencephalography, wPLI, Machine Learning, SHAP Analysis

Posted Date: November 23rd, 2026

DOI: https://doi.org/10.21203/rs.3.rs-10929075/v1

License: This work is licensed under a Creative Commons Attribution 4.0 International License.
Read Full License

Additional Declarations: No competing interests reported.

TitlePage

Resting-State MEG Functional Connectivity Changes in Lumbar Spinal Stenosis: A Multi-Band wPLI and Machine Learning Study

Authors:

Geng Zhao[1,2], Zhuang Miao[1,2], Xiaoxiong Wang[2], Hongwei Wang[3], Shiqiang Zheng[1], Xinyu Liu[2], Xu Zhang[1]

Affiliations:

[1] School of Instrumentation and Optoelectronic Engineering, Beihang University, Beijing, China

[2] Department of Orthopedics, Qilu Hospital of Shandong University, Jinan, China

[3] College of Medical Information and Artificial Intelligence, Shandong First Medical University, Jinan, China

Email address:

Geng Zhao, by2243211@buaa.edu.cn; Zhuang Miao, by2243212@buaa.edu.cn; Xiaoxiong Wang, cjwdkwyxxx@163.com; Hongwei Wang, wanghongwei04@gmail.com; Shiqiang Zheng, zhengshiqiang@buaa.edu.cn; Xinyu Liu, newyuliu@163.com; Xu Zhang, zhang_xu@buaa.edu.cn

Abstract

Purpose of the Study: To investigate alterations in resting-state brain functional connectivity in lumbar spinal stenosis (LSS) patients and to evaluate multi-band connectivity features between LSS patients and healthy controls (HCs).

Materials and Methods: The study included 39 LSS patients and 31 HCs. Resting-state recordings were acquired using a 64-channel magnetoencephalography (MEG) system. After preprocessing, power spectral density (PSD) and functional connectivity matrices based on the weighted phase lag index (wPLI) were calculated across eight sensor-level regions of interest in four frequency bands (theta, alpha, beta, and gamma). Multiple machine learning model were applied for classification, and SHapley Additive exPlanations (SHAP) analysis was used to interpret the best-performing model.

Results: PSD was significantly lower in the LSS group than in the HC group across all four frequency bands after false discovery rate (FDR) correction. Conventional group comparisons revealed no connectivity differences that survived correction for multiple comparisons after FDR correction. In machine learning analysis, the random forest model achieved the best performance with a mean cross-validated area under the curve (AUC) of 0.723 ± 0.262. The key discriminative features identified involved cross-regional connectivity in the theta, beta, and gamma bands. SHAP analysis indicated that connectivity among the central, parietal/centroparietal, temporal, and frontal pole regions contributed most to classification.

Conclusions: Patients with LSS showed multi-band reduced PSD and abnormalities in resting-state brain functional connectivity. Machine learning models can capture these abnormal patterns to

distinguish patients from HCs. The key features involve connectivity between sensorimotor integration networks and higher-order control regions, indicating that LSS is accompanied by central brain network remodeling.

Key words: Lumbar Spinal Stenosis; Magnetoencephalography; wPLI; Machine Learning; SHAP Analysis

Introduction

Lumbar spinal stenosis (LSS) is a common degenerative spinal disorder characterized by the spinal canal narrowing and compression of neural structures, often leading to low back pain, lower body pain or numbness, neurogenic claudication, and functional limitation [1,2]. Despite substantial advances in imaging assessment and surgical treatment, its potential mechanisms remain incompletely understood [3]. In particular, structural abnormalities observed on imaging examinations do not always correlate closely with symptom severity [4], suggesting that central nervous system remodeling may contribute to the clinical manifestations of LSS [5].

Accumulating evidence indicates that chronic pain and long-term abnormal sensory input are associated with functional reorganization of the brain [6]. Such reorganization may involve oscillatory activity changes, disrupted network coordination, and compensatory changes in sensorimotor systems [7-9]. In patients with chronic spinal disorders, sustained input of abnormal signals, gait disturbance, and sensorimotor mismatch may reshape cortical information processing beyond the site of spinal pathology. Therefore, investigating brain network changes in patients with LSS may provide further insight into the pathophysiology of the disease.

Magnetoencephalography (MEG) has millisecond temporal resolution, enabling frequency-specific characterization of interregional functional coupling. It offers a noninvasive approach for examining the brain's network organization [10,11]. Among available connectivity metrics, the weighted phase lag index (wPLI) has been widely used because it quantifies phase synchronization while reducing the influence of zero-lag correlations and volume conduction effects [12,13].

Accordingly, multi-band resting-state MEG connectivity analysis may help reveal abnormal neural communication patterns in LSS patients.

Machine learning provides a useful framework for integrating high-dimensional connectivity features and evaluating their potential diagnostic values. Rather than focusing on isolated connections, machine learning models can analysis distributed patterns in multiple frequency bands and brain regions [14-16]. In addition, explainable artificial intelligence approaches such as SHAP can identify the features which contribute most strongly to model predictions, thereby improving the interpretability of connectivity-based classification [17,18].

In this study, we used resting-state 64-channel MEG recordings to investigate changes in brain functional connectivity between LSS patients and healthy controls. We hypothesized that patients with LSS would exhibit abnormalities in resting-state functional connectivity, and that multi-band wPLI features would provide discriminative information for classification.

Materials and Methods

2.1 Participants

This study included LSS patients who were admitted to the Department of Spinal Surgery in Qilu Hospital between March 2025 and October 2025, as well as healthy controls recruited from the community. The overall experimental workflow was shown in Figure 1. The study was conducted according to the Declaration of Helsinki and approved by the Ethics Committee of Qilu Hospital

(Approval No. KYLL-202312-015-1). All participants were informed of the relevant content of the study and provided written informed consent forms. Demographic and clinical information, including age, sex, and disease-related clinical indicators, was collected for subsequent analysis. Patients were excluded if they had a history of spinal surgery, other types of spinal disorders, other neurological or systemic diseases, or were unable to undergo MEG examination.

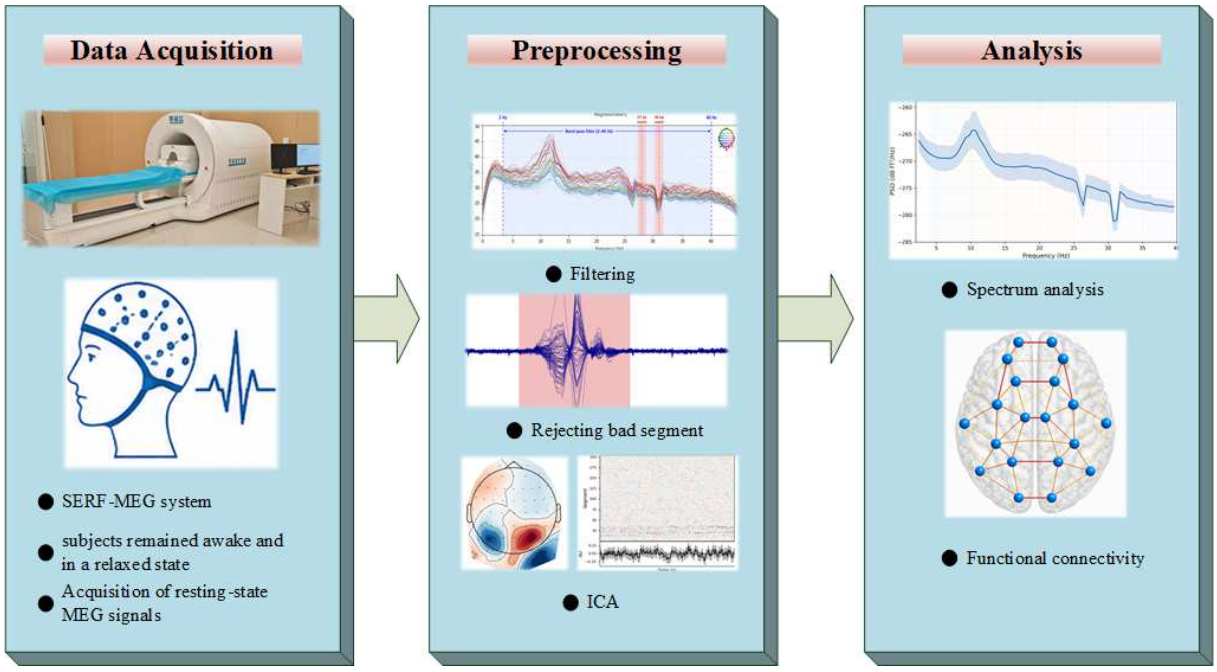

Figure 1. The experimental workflow of resting-state MEG analysis for lumbar spinal stenosis.

2.2 MEG acquisition

Resting-state MEG data were acquired using a 64-channel MEG system (Hangzhou Institute of Extremely-Weak Magnetic Field Major National Science and Technology Infrastructure, Hangzhou, ZJ, China). The sensitivity of OPM magnetometers was 20 $fT/\sqrt{\text{Hz}}$[19]. The positions of the magnetoencephalographic sensors were arranged in accordance with the international 10-20 system. All MEG recordings were performed in a magnetically shielded room where the residual magnetic

field intensity in the central area was lower than 10 nT. During the MEG examination, subjects were required to remain awake and relaxed, and physical movements were minimized as much as possible. A camera was used to monitor the safety of the subjects and ensure they did not fall asleep. During raw data reconstruction, sensor position and sensor orientation information were incorporated and organized together with the final continuous recording data.

2.3 Preprocessing of resting-state MEG

Bad channels were first inspected by power spectral density (PSD) visualization and manual review. The continuous data were then band-pass filtered between 2 and 40 Hz, followed by notch filtering at specific noise frequencies of 27 Hz and 30 Hz. To further reduce environmental interference, bias field correction based on projection operators was applied to the filtered MEG data. Subsequently, noisy time segments were automatically annotated using a z-score-based procedure, marking artifact-contaminated periods as bad segments for later exclusion. Independent component analysis (ICA) was used to identify ocular and electrocardiographic artifacts. The MEG data were segmented into 5-second epochs, and epochs containing bad segments were discarded.

2.4 Power spectral density analysis

For each participant, power spectral density was estimated from the artifact-cleaned resting-state MEG recording. PSD values were first averaged across all retained MEG channels to obtain an individual whole-brain spectrum, and then the PSD averaged across participants within each group. Group spectra are presented in decibels. Band-level power was evaluated for theta (4-8Hz), alpha (8-13Hz), beta (13-30Hz), and gamma (30-40Hz) bands.

2.5 Functional connectivity analysis and feature construction

ROI-level wPLI matrices were calculated in the theta, alpha, beta, and gamma bands. ROIs were defined at the sensor level by grouping the 64 sensor channels into eight ROIs: Occipital, Parietal, Central, Centroparietal, Frontal, FrontalPole, Temporal, and Frontocentral. Functional connectivity features were extracted at the individual subject level. The the final feature set consisted of multi-band wPLI connectivity features corresponding to the theta, alpha, beta, and gamma bands.

2.6 Machine learning framework

Based on subject-level wPLI features, a multi-model machine learning framework was used to classify patients with LSS and HCs. The models included logistic regression, support vector machine (SVM), random forest (RF), k-nearest neighbors (KNN), naive Bayes (NB), decision tree (DT), and logistic regression (LR). To avoid information leakage and obtain unbiased estimates of model performance, nested group-aware cross-validation was adopted. Subject identifiers were used as grouping variables to ensure that data from the same participant were not split between training and test sets. The outer loop was used for performance evaluation, whereas the inner loop performed hyperparameter tuning by grid search.

2.7 SHAP analysis

To improve the interpretability, SHAP analysis was performed for the best-performing model. SHAP values were summarized using the mean absolute contribution of each feature. This approach enabled identification of the connectivity features which contributed most strongly to the classification of LSS and HCs.

2.8 Statistical analysis

Descriptive statistics were used to summarize demographic and clinical variables. Between-group comparisons of band-averaged PSD were performed using Welch independent t-tests. *P* values for the four PSD bands were corrected using the false discovery rate (FDR) procedure. Individual connectivity features were compared between groups, with FDR correction applied within each frequency band. Machine learning performance across outer folds was reported as mean ± standard deviation, and the primary endpoint for model comparison was AUC. Statistical significance was set at $p < 0.05$.

Results

3.1 Participant characteristics

A total of 39 LSS patients and 31 HCs were included in the final analysis. The demographic and clinical characteristics of the participants are summarized in Table 1 and Table 2. There were no significant differences between the two groups in age ($p = 0.146$) or sex ($p = 0.855$).

Table 1 Demographic data and function scores

	HC	LSS
Age	58.9±7.2	55.5±12.9
Sex (male/female)	15/16	18/21
Height (cm)	164.3 ± 7.2	165.2 ± 8.7
Weight (kg)	64.2±8.8	67.2±10.9

Table 2 Clinical data and function scores of LSS patients

	LSS
During of symptoms (months)	31.0±30.1
Involved segments	1.5±0.7
JOA score	19.1±3.9
SF-36 score	
PF, physical function	41.0±21.9
RP, role physical	33.3±29.9
BP, bodily pain	39.7±21.1
GH, general health	28.2±17.8
VT, vitality	49.4±18.6
SF, social function	48.4±16.0
RE, role emotional	45.3±34.6
MH, mental health	50.2±15.9

3.2 Power spectral density

The resting-state PSD of the LSS and HC groups are shown in Figure 2. Both groups displayed similar spectral shapes. However, the LSS curve was consistently lower than the HC curve. Band analysis showed that the PSD of the LSS group across all four frequency bands was significantly lower than that of the HC group after FDR correction (theta band $p_{adj}<0.001$, alpha band $p_{adj}= 0.006$, beta band $p_{adj}= 0.013$, and gamma band $p_{adj}= 0.030$)

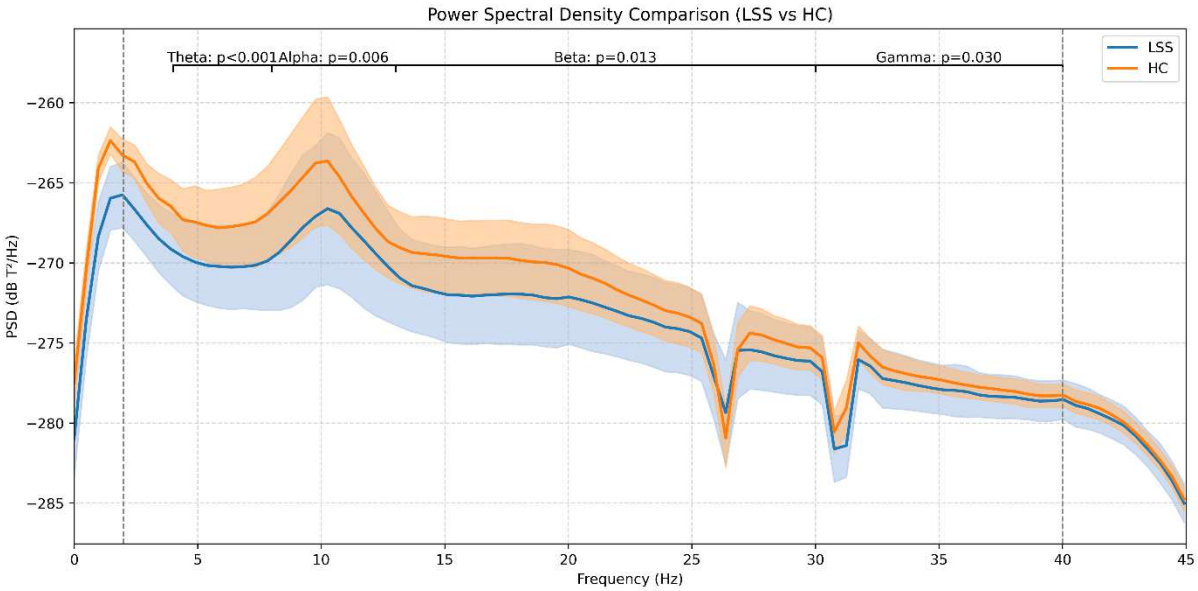

Figure 2. Whole-brain power spectral density profiles in patients with LSS and healthy vulunteers. Solid lines represent group means and shaded areas represent standard deviations.

3.2 Overview of multi-band resting-state functional connectivity features

Group comparisons based on ROI-level wPLI are shown in Figure 3. Significant between-group differences were mainly distributed across the theta, alpha, and gamma bands. In the theta band, the main differences involved Centroparietal-FrontalPole and Centroparietal-Frontal connectivity. In the alpha band, the main differences involved Central-FrontalPole, Occipital-Centroparietal, and Occipital-Parietal connectivity. In the gamma band, the main differences were primarily concentrated in Centroparietal-FrontalPole and Central-Centroparietal connectivity. However, none of these connections remained significant after FDR correction for multiple comparisons across all ROI pairs in each band. The minimum corrected *p* values in the theta, alpha, and gamma bands were 0.142, 0.147, and 0.120, respectively.

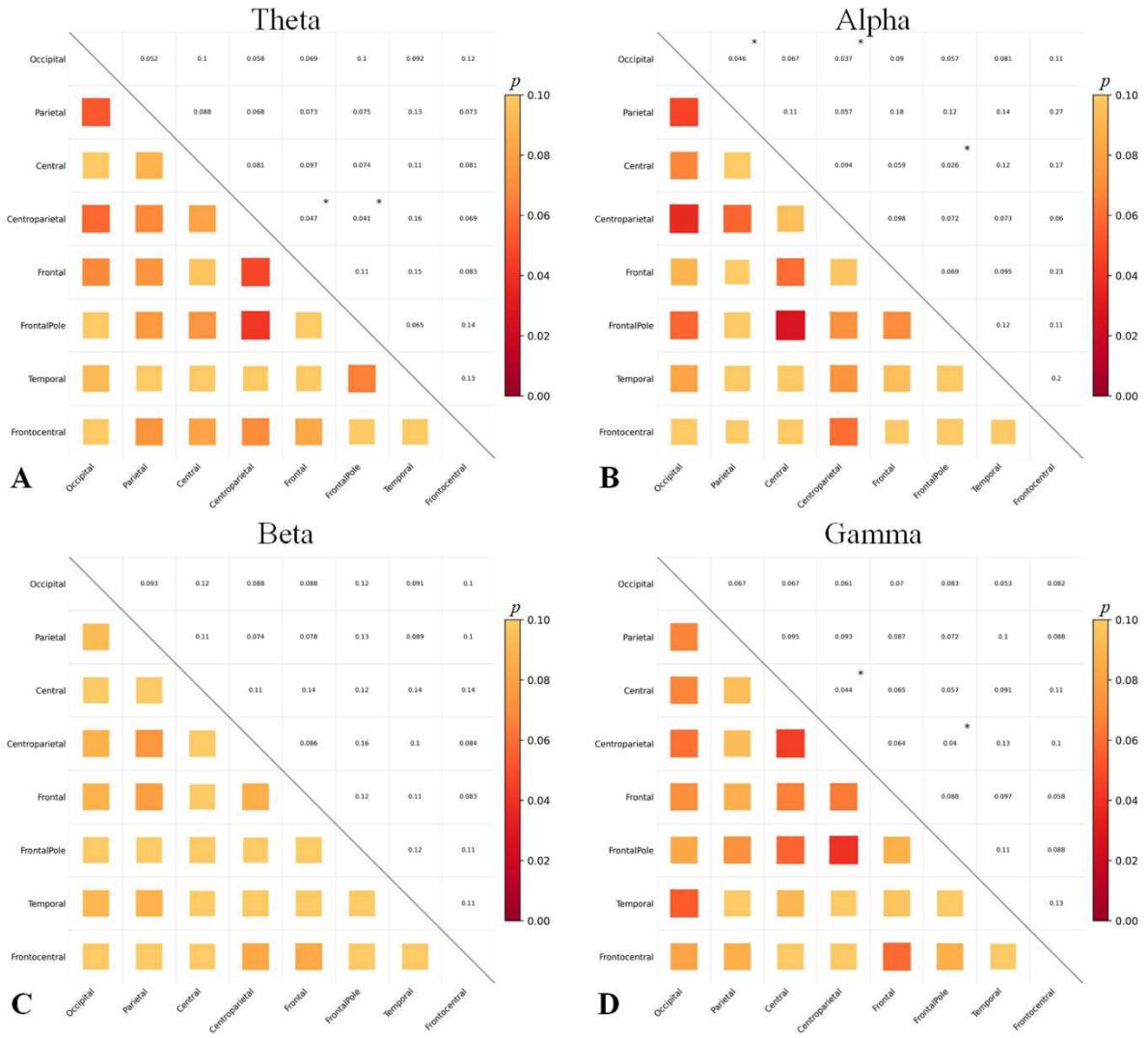

Figure 3. *p* values for wPLI differences between the LSS and HC groups in the theta, alpha, beta, and gamma frequency bands.

3.3 Performance of the machine learning models

Multiple machine learning models were compared using nested group cross-validation based on multi-band wPLI functional connectivity features. As shown in Figure 4, the random forest model achieved the best performance, with a mean AUC of 0.723 ± 0.262, an accuracy of 0.681 ± 0.186, a balanced accuracy of 0.678 ± 0.198, and an F1 score of 0.744 ± 0.138. The k-nearest neighbors and

naive Bayes models ranked next, with AUCs of 0.713 ± 0.219 and 0.711 ± 0.226, respectively. Logistic regression showed moderate performance, with an AUC of 0.685 ± 0.075. The decision tree model performed slightly worse, with an AUC of 0.655 ± 0.224. The SVM model showed the weakest overall performance on the current feature set, with an AUC of 0.514 ± 0.362. Overall, several models demonstrated some degree of discriminative ability, but the random forest model showed relatively superior performance and overall stability.

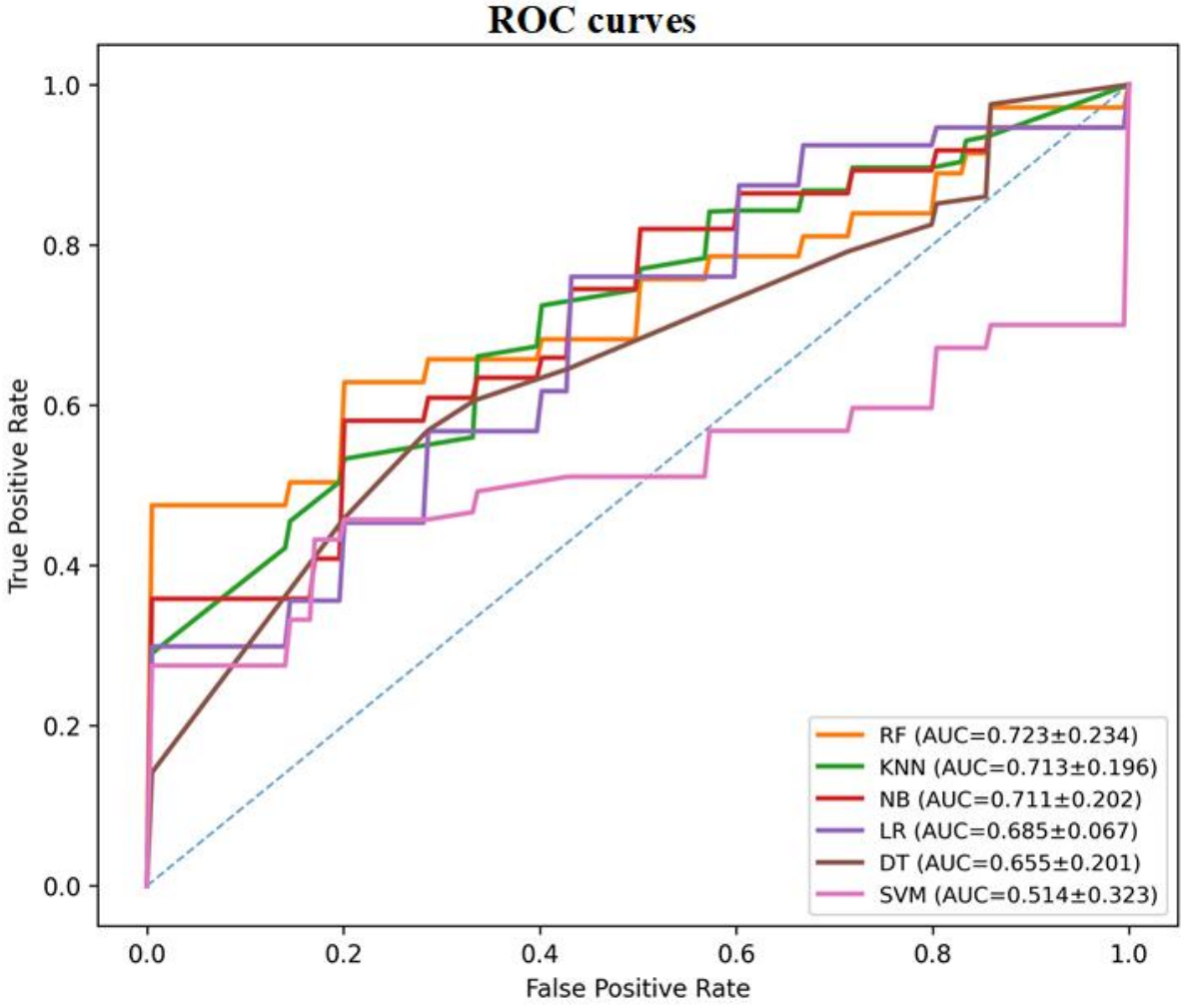

Figure 4. ROC curves of the machine learning approaches. ROC, receiver operating characteristic.

3.4 SHAP-based interpretation of discriminative connectivity features

As shown in Figure 5, SHAP analysis revealed the connectivity features that contributed most strongly to the random forest classification decisions. Frontal pole-related connections were particularly prominent in the beta and gamma bands, whereas theta-band Central-Temporal, Parietal-Temporal, and Occipital-Centroparietal connectivity also made substantial contributions. The direction of the effects of different feature values on model output was clear, but not entirely consistent across features. Higher values of Beta-Central-FrontalPole were more frequently distributed in the positive SHAP region, suggesting that increased connectivity in this feature tended to push the model output toward the patient class. In contrast, for features such as Gamma-Central-Centroparietal and Gamma-Parietal-Central, higher or lower feature values corresponded to opposite contribution directions. Overall, the SHAP results suggest that model discrimination depended mainly on some highly contributive cross-regional connections.

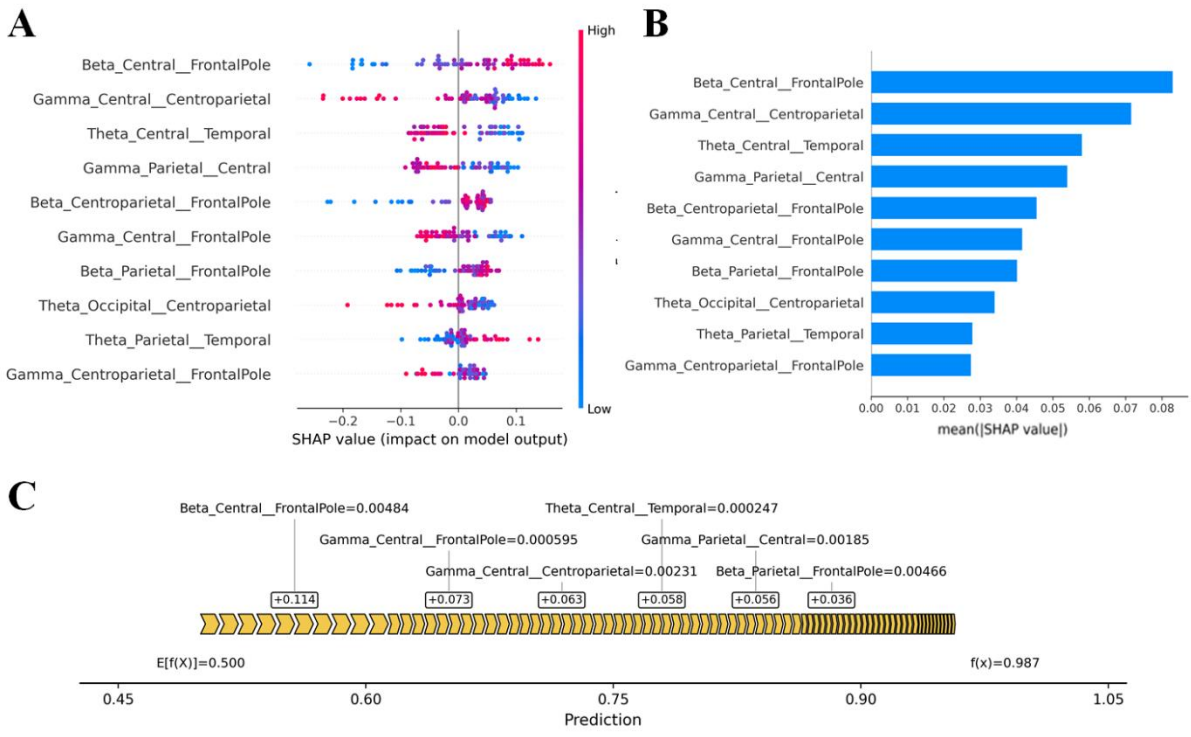

Figure 5. SHAP values for the RF model. (A) SHAP summary plot; (B) SHAP waterfall plot; (C) SHAP force plot. RF, random forest; SHAP, SHapley Additive exPlanations.

Discussion

Based on resting-state PSD and multi-band wPLI functional connectivity features from MEG, this study combined SHAP interpretability analysis to investigate central neurophysiological changes in LSS patients. First, LSS patients showed significantly lower whole-brain PSD in the theta, alpha, beta, and gamma bands. Second, subject-level resting-state functional connectivity features could be stably extracted. Third, the machine learning models demonstrated some degree of discriminative ability, among which the RF model achieved the best overall performance. Finally, SHAP analysis identified highly informative cross-regional connectivity features that contributed most strongly to classification.

A strength of this study is the combined use of both traditional statistical comparison methods and multivariate machine learning approaches. Conventional comparisons showed several differences between LSS and healthy controls at the uncorrected level in the four bands; however, no differences remained significant after FDR correction. This suggests that the changes with LSS patients in brain functional connectivity are more likely to manifest as distributed, small-effect network patterns rather than a few isolated connections that remain highly significant.

LSS is a degenerative spinal disease characterized by chronic pain, abnormal sensory and motor function, and restricted gait [3,20]. Although the direct injury is located in the lumbar spine, long-term chronic symptoms can further affect the information integration of the central nervous system. [6,21].

The key connections in this study were not confined to a single local brain region but were distributed between sensorimotor-related areas and higher association regions. That suggested that LSS-related abnormalities might related to wide network remodeling rather than simple region changes. The central, parietal, and centroparietal cortices play important roles in somatosensory integration, postural control, and sensorimotor transformation [22-24]. The persistent abnormalities with LSS patients in sensory input and sensorimotor feedback may further influence information integration and synchronous activity in brain networks [25].

In the current sample, the random forest model achieved the best performance, indicating that multi-band resting-state MEG functional connectivity features have the ability to distinguish patients with LSS from healthy individuals. The top SHAP features repeatedly involved frontal pole connectivity as well as central, centroparietal, and temporal connections, suggesting that the central network changes of LSS may involve both sensorimotor networks and higher regulatory networks. In particular, the high contributions of Beta-Central-FrontalPole, Beta-Centroparietal-FrontalPole, and Gamma-Central-FrontalPole suggest that the frontal pole is not only passively involved, but may actively participate in chronic pain adaptation, internal state monitoring, and motor strategy regulation. At the same time, the importance of Theta-Central-Temporal and Theta-Parietal-Temporal suggests that abnormalities of LSS are not limited in prefrontal-sensorimotor pathways, but also involve broader integration processes.

This study still has several limitations. First, the sample size was relatively limited, and no independent external validation cohort was available. Therefore, the current model performance requires further verification in larger samples. Second, the study was based on ROI-level functional

connectivity analysis, which improves stability and interpretability but provides low spatial resolution and cannot replace source-space analysis. Third, the cross-sectional design does not allow determination of whether the observed brain network changes are consequences of disease progression or reflect susceptibility in some participants. Finally, although SHAP provides a useful framework for model interpretation, its results remain dependent on the current training data and model structure, and further validation with independent datasets is still needed.

Conclusions

This study demonstrates that patients with LSS exhibit significant reductions in resting-state PSD, and detectable distributed multi-band abnormalities in functional connectivity. Machine learning models based on ROI-level wPLI features were able to distinguish patients from healthy controls. SHAP analysis further showed that the connectivity among the central, parietal, centroparietal, temporal, and frontal pole regions constituted the key features driving classification decisions. These findings suggest that LSS is not only a structural disorder of the peripheral and spinal systems but is also accompanied by distributed central brain network remodeling. Multi-band resting-state MEG functional connectivity features may therefore provide a new basis for understanding its neural mechanisms and for exploring objective imaging biomarkers.

Declarations

Ethics approval and consent to participate

This study was approved by the Ethics Committee of Qilu Hospital (Approval No. KYLL-202312-015-1). All participants were fully informed about the study details and provided informed consent.

Consent for publication

Not applicable

Availability of data and materials

The datasets of the current study are not publicly available due to patient privacy concerns but are available from the corresponding author on reasonable request.

Competing interests

The authors declare that they have no competing interests

Funding

This study is supported by the Key R&D Program of Shandong Province (Grant number: 2022ZLGX03) and the Fundamental and Interdisciplinary Disciplines Breakthrough Plan of the Ministry of Education of China (Grant number: JYB2025XDXM606)

Authors' contributions

G.Z. contributed to the conception of the work and wrote the main manuscript; X.W.and X. L. contributed to the acquisition of data; G.Z., Z.M. and H.W. contributed to data analysis; S. Z., X.Z. and X. L. contributed to agree to be accountable for all aspects of the work. All authors reviewed the manuscript.

Acknowledgements

Not applicable

Reference：

1. Katz JN, Zimmerman ZE, Mass H, Makhni MC. Diagnosis and Management of Lumbar Spinal Stenosis: A Review. JAMA. 2022;327(17):1688-1699. doi: 10.1001/jama.2022.5921.
2. Covaro A, Vilà-Canet G, de Frutos AG, Ubierna MT, Ciccolo F, Caceres E. Management of degenerative lumbar spinal stenosis: an evidence-based review. EFORT Open Rev. 2017;1(7):267-274. doi: 10.1302/2058-5241.1.000030.
3. Kwon JW, Moon SH, Park SY, et al. Lumbar Spinal Stenosis: Review Update 2022. Asian Spine J. 2022;16(5):789-798. doi: 10.31616/asj.2022.0366.
4. Andrasinova T, Adamova B, Buskova J, Kerkovsky M, Jarkovsky J, Bednarik J. Is there a Correlation Between Degree of Radiologic Lumbar Spinal Stenosis and its Clinical Manifestation? Clin Spine Surg. 2018;31(8):E403-E408. doi: 10.1097/BSD.0000000000000681.
5. Güneş M, Apaydın AS. The relationship of central sensitization with disability, pain catastrophizing, depression, and sleep quality in patients with lumbar spinal stenosis. J Orthop Sci. 2026. doi: 10.1016/j.jos.2026.02.013.
6. Henry DE, Chiodo AE, Yang W. Central nervous system reorganization in a variety of chronic pain states: a review. PM R. 2011;3(12):1116-1125. doi: 10.1016/j.pmrj.2011.05.018.
7. Ploner M, Sorg C, Gross J. Brain Rhythms of Pain. Trends Cogn Sci. 2017;21(2):100-110. doi: 10.1016/j.tics.2016.12.001.
8. Zebhauser PT, Hohn VD, Ploner M. Resting-state electroencephalography and magnetoencephalography as biomarkers of chronic pain: a systematic review. Pain. 2023;164(6):1200-1221. doi: 10.1097/j.pain.0000000000002825.

9. May ES, Nickel MM, Ta Dinh S, et al. Prefrontal gamma oscillations reflect ongoing pain intensity in chronic back pain patients. Hum Brain Mapp. 2019;40(1):293-305. doi: 10.1002/hbm.24373.
10. Brookes MJ, Woolrich M, Luckhoo H, et al. Investigating the electrophysiological basis of resting state networks using magnetoencephalography. Proc Natl Acad Sci U S A. 2011;108(40):16783-16788. doi: 10.1073/pnas.1112685108.
11. Hipp JF, Hawellek DJ, Corbetta M, Siegel M, Engel AK. Large-scale cortical correlation structure of spontaneous oscillatory activity. Nat Neurosci. 2012;15(6):884-890. doi: 10.1038/nn.3101.
12. Vinck M, Oostenveld R, van Wingerden M, Battaglia F, Pennartz CM. An improved index of phase-synchronization for electrophysiological data in the presence of volume-conduction, noise and sample-size bias. Neuroimage. 2011;55(4):1548-1565. doi: 10.1016/j.neuroimage.2011.01.055.
13. Imperatori LS, Betta M, Cecchetti L, et al. EEG functional connectivity metrics wPLI and wSMI account for distinct types of brain functional interactions. Sci Rep. 2019;9(1):8894. doi: 10.1038/s41598-019-45289-7.
14. Nenning KH, Langs G. Machine learning in neuroimaging: from research to clinical practice. Radiologie (Heidelb). 2022;62(Suppl 1):1-10. doi: 10.1007/s00117-022-01051-1.
15. Avery EW, Yoo K, Rosenberg MD, et al. Distributed Patterns of Functional Connectivity Predict Working Memory Performance in Novel Healthy and Memory-impaired Individuals. J Cogn Neurosci. 2020;32(2):241-255. doi: 10.1162/jocn_a_01487.

16. Nielsen AN, Barch DM, Petersen SE, Schlaggar BL, Greene DJ. Machine Learning With Neuroimaging: Evaluating Its Applications in Psychiatry. Biol Psychiatry Cogn Neurosci Neuroimaging. 2020;5(8):791-798. doi: 10.1016/j.bpsc.2019.11.007.
17. Lundberg SM, Erion G, Chen H, et al. From Local Explanations to Global Understanding with Explainable AI for Trees. Nat Mach Intell. 2020;2(1):56-67. doi: 10.1038/s42256-019-0138-9.
18. Amoroso N, Quarto S, La Rocca M, Tangaro S, Monaco A, Bellotti R. An eXplainability Artificial Intelligence approach to brain connectivity in Alzheimer's disease. Front Aging Neurosci. 2023;15:1238065. doi: 10.3389/fnagi.2023.1238065.
19. Wang F, Ma Y, Gao T, et al. Repairbads: An automatic and adaptive method to repair bad channels and segments for OPM-MEG. Neuroimage. 2025;306:120996. doi: 10.1016/j.neuroimage.2024.120996.
20. Deer T, Sayed D, Michels J, Josephson Y, Li S, Calodney AK. A Review of Lumbar Spinal Stenosis with Intermittent Neurogenic Claudication: Disease and Diagnosis. Pain Med. 2019;20(Suppl 2):S32-S44. doi: 10.1093/pm/pnz161.
21. Vittersø AD, Halicka M, Buckingham G, Proulx MJ, Bultitude JH. The sensorimotor theory of pathological pain revisited. Neurosci Biobehav Rev. 2022;139:104735. doi: 10.1016/j.neubiorev.2022.104735.
22. Buneo CA, Andersen RA. The posterior parietal cortex: sensorimotor interface for the planning and online control of visually guided movements. Neuropsychologia. 2006;44(13):2594-2606. doi: 10.1016/j.neuropsychologia.2005.10.011.
23. Jacobs JV, Horak FB. Cortical control of postural responses. J Neural Transm (Vienna). 2007;114(10):1339-1348. doi: 10.1007/s00702-007-0657-0.

24. Gombaut C, Holmes SA. Sensorimotor Integration and Pain Perception: Mechanisms Integrating Nociceptive Processing. A Systematic Review and ALE-Meta Analysis. Front Integr Neurosci. 2022;16:931292. doi: 10.3389/fnint.2022.931292.

25. Houle M, Bonneau JD, Marchand AA, Descarreaux M. Physical and Psychological Factors Associated With Walking Capacity in Patients With Lumbar Spinal Stenosis With Neurogenic Claudication: A Systematic Scoping Review. Front Neurol. 2021;12:720662. doi: 10.3389/fneur.2021.720662.